Icarus 260 (2015) 94–102

Contents lists available at ScienceDirect

Icarus

journal homepage: www.elsevier.com/locate/icarus

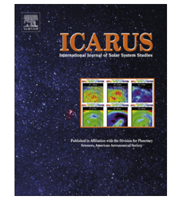

Thermal imaging of Uranus: Upper-tropospheric temperatures one season after Voyager

Glenn S. Orton [a,*], Leigh N. Fletcher [b], Therese Encrenaz [c], Cedric Leyrat [c], Henry G. Roe [d], Takuya Fujiyoshi [e], Eric Pantin [f]

[a] MS 183-501, Jet Propulsion Laboratory, California Institute of Technology, 4800 Oak Grove Drive, Pasadena, CA 91109, USA
[b] Atmospheric, Oceanic & Planetary Physics, Department of Physics, University of Oxford, Clarendon Laboratory, Parks Road, Oxford OX1 3PU, United Kingdom
[c] LEISA, Observatoire de Paris, F-92195 Meudon, France
[d] Lowell Observatory, 1400 West Mars Hill Road, Flagstaff, AZ 86001, USA
[e] Subaru Telescope, National Astronomical Observatory of Japan, National Institutes of Natural Sciences, 650 N. A'ohoku Place, Hilo, HI 96720, USA
[f] Centre d'Études Atomiques, Saclay, 91109 Gif-sur-Yvette, France

A R T I C L E I N F O

Article history:
Received 16 February 2015
Revised 24 June 2015
Accepted 9 July 2015
Available online 16 July 2015

Keywords:
Uranus
Uranus, atmosphere
Jovian planets
Atmospheres, structure

A B S T R A C T

We report on 18–25 μm thermal imaging of Uranus that took place between 2003 and 2011, a time span roughly one season after the thermal maps made by the Voyager-2 IRIS experiment in 1986. We re-derived meridional variations of temperature and *para*-H_2 fraction from the Voyager experiment and compared these with the thermal images, which are sensitive to temperatures in the upper troposphere of Uranus around the 70–400 mbar atmospheric pressure range. The thermal images display a maximum of 3 K of equivalent temperature changes across the disk, and they are consistent with the temperature distribution measured by the Voyager IRIS experiment. This implies that there has been no detectable change of the meridional distribution of upper-tropospheric/lower-stratospheric temperatures over a season. This is inconsistent with seasonally dependent radiative–convective-dynamical models and full global climate models that predict some variability with season if the effective temperature is meridionally constant. We posit that the effective temperature of Uranus could be meridionally variable, with the additional possibility that even the small temperature variations predicted by the GCMs are overestimated.

1. Introduction

With its 98° rotational axis tilt from its orbital plane, the atmosphere of Uranus is subject to extremes of seasonal variability in 84-year cycles of daylight and darkness. The thermal structure and response of the atmosphere to these extremes were determined only once in 1986 with close-up thermal spectroscopy of Uranus by the Voyager-2 IRIS experiment (e.g. Flasar et al., 1987; Conrath et al., 1990). It measured the north pole near winter solstice (planetocentric solar longitude $L_s = 273°$) in the midst of its long winter darkness, yielding upper tropospheric (80-mbar) temperatures that were 1–2 K warmer than at the equator (Conrath et al., 1998). In order to determine the effect of extremes of variable sunlight on different latitudes in Uranus, we needed to determine temperatures near the same upper-troposphere levels as measured by the IRIS experiment. This is not possible from Earth using the same 30–50 μm wavelength range as the Voyager IRIS experiment because of strong absorption by water vapor in our own atmosphere. However, we can measure temperatures in a portion of the 75–650 mbar pressure range covered by the Voyager IRIS experiment from the 18–25 μm spectral range that is accessible from ground-based observatories. The IRIS experiment was also sensitive to the relative abundances of *para*-H_2 vs. *ortho*-H_2 ratio, parameterized by the *para*-H_2 fraction, whose departures from local equilibrium can serve as a tracer of vertical motion. Ground-based observations that extend to 25 μm are also sensitive to the *para*-H_2 fraction at one level, around 200 mbar of atmospheric pressure. We report here Earth-based spatially resolved thermal images of Uranus between 18 and 25 μm taken between 2003 and 2011 ($L_s = 354–14°$). Following the Voyager IRIS measurements by 17–25 years, they map upper-tropospheric temperatures and the *para*-H_2 fraction at a significantly different season than Voyager, near the northern spring equinox ($L_s = 0°$).

* Corresponding author.

http://dx.doi.org/10.1016/j.icarus.2015.07.004

2. Observations

We assume that molecular hydrogen (H_2) is well mixed in the atmosphere of Uranus, because the spectral region we sample is insensitive to the condensation level of CH_4 whose unsaturated mixing ratio in the deeper atmosphere could be as high as 4% (Lindal et al., 1987; Rages et al., 1991; Sromovsky et al., 2011). Thus, variability in observed radiances from regions dominated by the opacity of H_2 can be used to determine the variability of temperatures. Fig. 1 illustrates that the 17–25 μm spectrum of Uranus is dominated by the collision-induced opacity of H_2. Fig. 2 displays contribution functions that illustrate that this spectral range is sensitive to the vertical temperature structure in the pressure range of 70–400 mbar. Furthermore, it is also sensitive to the *para*-H_2 fraction because the collision-induced absorption in this region is composed of contributions of the broad rotational features arising from the S(0) (*para*-H_2) and S(1) (*ortho*-H_2) transitions. Thus, an intercomparison of radiances from these wavelengths can determine the *para*-H_2 fraction and its variability at 50–300 mbar pressures over different latitudes in Uranus. Although there are intervals in the 9–11 μm region that may well be dominated by very weak H_2 collision-induced absorption and are thus sensitive to temperatures as deep as the 2-bar pressure level (see Orton et al., 2014b), radiances in that region are much weaker and their detection from ground-based facilities is impractical.

Images of Uranus were obtained with filters associated with the mid-infrared facility instruments shown in Table 1, which also summarizes the details of each observing run. Fig. 3 displays the final image products. All images were made with standard chopping and nodding in order to subtract background sky emission on time scales of seconds and minutes, respectively. All the images were made in association with other targets for each night, and the required integration and associated overhead times made it impossible to observe the planet using more than one filter per night. The sequence of the observations was driven by a combination of the overhead water–vapor burden (a low value permitted longer-wavelength observations) and what had already been observed, starting with what we judged to be the easiest detections.

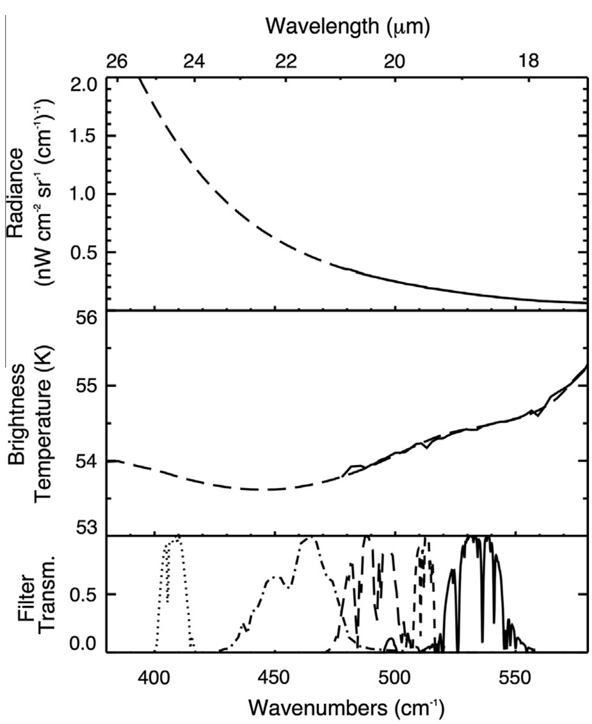

Fig. 1. Normalized transmission function of filters relative to the radiance and brightness-temperature spectrum of Uranus. The transmission functions include consideration of telluric absorption, assuming a precipitable water vapor depth of 1 mm. From right to left, the filter functions represent the filters denoted as 18.7 μm (solid line), 19.6 μm (short-dashed line), 20.3 μm (long dashed line), 22.0 μm (dash-dotted line) and 24.5 μm (dotted line). Table 1 summarizes the circumstances of the observations with each filter. The solid line in the radiance and brightness-temperature plots is the disk-averaged spectrum of Uranus from the long-low mode of Spitzer IRS observations (Orton et al., 2014b). The dashed line is the extension of that spectrum to longer wavelengths using a model that fits the IRS data best. This model assumes a *para*-H_2 fraction that is at equilibrium at the local temperature.

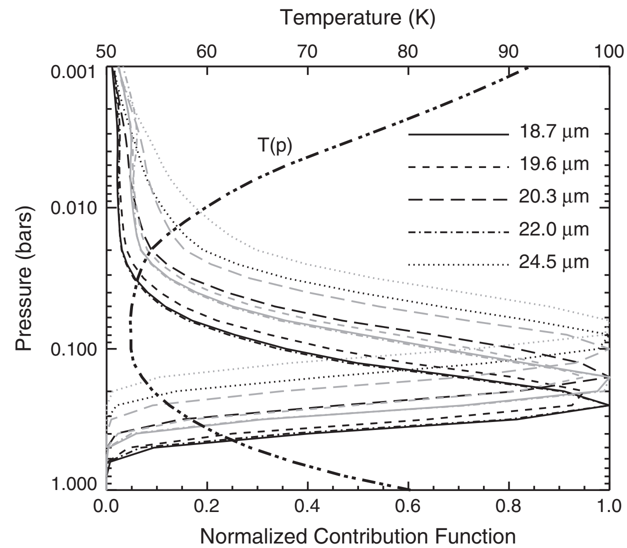

Fig. 2. Vertical contribution functions corresponding to the filters shown in Fig. 1. Black curves are for emission observed at the nadir, and gray curves are for emission observed at an emission angle of 48°, the highest angle that we estimate that observations at the longest wavelength (24.5 μm) detects the planet near the limb without significant contributions from dark space past the limb. The line styles are the same as used in Fig. 1. The triple-dotted-dashed curve represents the assumed temperature profile, taken from Orton et al. (2014b).

Table 1
Summary of Uranus observations.

Central wavelength (FWHM of filter)	Source	UT date	Start–end times (UTC)
18.7 μm (0.83 μm)	VLT/VISIR	2006 Sep. 2	4:29–7:21
18.7 μm (0.83 μm)	VLT/VISIR	2006 Sep. 3	4:03–6:35
19.5 μm (0.35 μm)	VLT/VISIR	2009 Aug. 27	5:48–10:06
20.5 μm (0.97 μm)	Subaru/ COMICS	2011 Aug. 27	11:34–11:54
22.0 μm (1.60 μm)	Keck/LWS	2003 Jul. 20	13:49–14:53
24.5 μm (0.16 μm)	Subaru/ COMICS	2008 Sep. 15	9:16–9:51
24.5 μm (0.16 μm)	Subaru/ COMICS	2008 Sep. 16	8:27–9:31

2.1. 18.7 μm

Some of our initial thermal images of Uranus were made with an 18.7-μm filter during the second half of two nights on the Very Large Telescope (VLT) UT3, using the VISIR instrument (Lagage et al., 2004). Some images on 2006 Sep. 2 were acquired after 7:21 UT but ultimately discarded because of degraded